Struct Chem (2016) 27:209–219
DOI 10.1007/s11224-015-0693-6

ORIGINAL RESEARCH

Conformations, vibrational spectra and force field of 1-methyl-2-(2′-pyridyl)benzimidazole: experimental data and density functional theory investigation in comparison with 2-(2′-pyridyl)benzimidazole

G. M. Kuramshina[1] · O. A. Vakula[1] · N. I. Vakula[1] · A. G. Majouga[1] · V. M. Senyavin[1] · Leonid G. Gorb[2] · Jerzy Leszczynski[2]

Received: 27 October 2015 / Accepted: 29 October 2015 / Published online: 18 November 2015

Abstract The molecular structure, conformational equilibria, vibrational spectra and molecular force field of 1-methyl-2-(2′-pyridyl)benzimidazole have been determined at the HF, MP2 and DFT/(B3LYP, BVP86) levels with 6-31+G(d,p) and TZVP basis sets. The torsional potentials for the rotation around the C1–C2 pivotal bond have been calculated at the B3LYP/6-31+G(d,p) and BVP86/TZVP levels of theory for gaseous and aqueous 1-methyl-2-(2′-pyridyl)benzimidazole. FT-Raman (3500–10 cm^{-1}) and FT-IR (3900–400 cm^{-1}) spectra of solid 1-methyl-2-(2′-pyridyl)benzimidazole have been recorded and interpreted on a base of calculated potential energy distribution. The results of the experimental and theoretical study of vibrational spectra and molecular structure of 1-methyl 2-(2′-pyridyl)benzimidazole are considered in comparison with similar data for 2-(2′-pyridyl)benzimidazole.

Keywords 1-Methyl-(2′-pyridyl)benzimidazole (1-methyl-2-pyridin-2-yl-1H-benzimidazole) · Conformation · FT-IR and FT-Raman spectra · DFT · Torsional potential

Introduction

2PBI is an important heterocyclic bioactive compound widely used in the coordination chemistry, pharmacology and industry and to model important biological systems. Derivatives of the 2-(2′-pyridyl)benzimidazole (2PBI) have recently received much attention [1–7] due to the proton-transfer reactions in the exited states of these compounds. Sulfur-containing derivatives of 2PBI can serve as a very effective protection of various metal nanoparticles [8, 9]. Another interesting property of 2PBI and its alkyl derivatives is their ability to bind to the surface of metal nanoparticles, particularly gold nanoparticles, and to prevent them from aggregation and harsh reaction conditions [10]. The knowledge of the molecular structure and conformational preferences of 2PBI derivatives is necessary for the identification of photoreaction products as well as for clarifications of the proton-transfer reactions mechanism.

However, to the authors' best knowledge, a complete vibrational study of alkyl-substituted 2-(2′-pyridyl)benzimidazole has not been reported and conformational stabilities have not been investigated. An assignment of vibrational spectra of 2PBI which have been proposed in Ref. [11] was entirely based on the experimental IR and Raman data. DFT (B3LYP/6-311+G*) calculations of 2PBI possible conformations have been carried out in Ref. [12] for supporting the laser-induced fluorescence and IR-UV double resonance spectroscopy investigations of the H_2O and MeOH complexes of 2PBI, but no detailed quantum mechanical predictions of vibrational spectra of stable conformations have been carried out. The structure of solid 2PBI has been determined by the X-ray diffraction [13]. Recently, the effect of microhydration on the structure and vibrational spectra of 2PBI and 1-methyl-2-(2′-

Electronic supplementary material The online version of this article (doi:10.1007/s11224-015-0693-6) contains supplementary material, which is available to authorized users.

✉ G. M. Kuramshina
kuramshi@phys.chem.msu.ru

[1] Department of Physical Chemistry, Faculty of Chemistry, Lomonosov Moscow State University, Moscow, Russia 119991

[2] Department of Chemistry, ICNANOTOX, Jackson State University, Jackson, MS 39217, USA

pyridyl)benzimidazole (Me2PBI) has been investigated at B3LYP/6-31+G(d,p) level of theory [14].

The objectives of this work were to carry out the experimental investigation of FT-IR and FT-Raman spectra of 1-methyl-2-(2′-pyridyl)benzimidazole (Me2PBI) simplest alkyl derivative of 2PBI specially synthesized for this investigation, and to study theoretically the molecular structure, torsional potentials, IR and Raman spectra of Me2PBI with a goal to analyze the influence of alkyl substitution on molecular conformation and vibrational spectra in comparison with 2PBI. The molecule of Me2PBI can exist in two tautomeric forms, and one of them adopts two conformations A and B (Fig. 1). Me2PBI-A and Me2PBI-B are rotamers; structure C is the second tautomeric form. It is known that 2PBI molecule exists in the similar conformations [12], but according to the investigation of absorption spectra in a wide variety of solvents [2–4], 2PBI-C form is absent in the ground state.

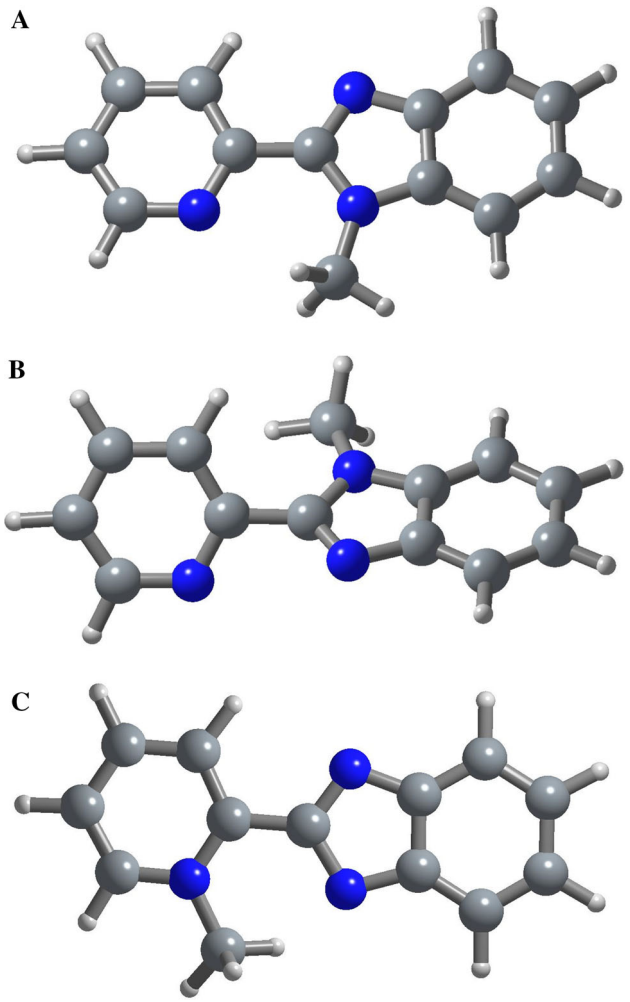

Fig. 1 Stable conformations of 1-methyl 2-(2′-pyridyl)benzimidazole molecule

The optimized geometries of all possible conformations, harmonic force fields, IR intensities and Raman activities of stable conformations of Me2PBI in gaseous state have been obtained at the different theoretical levels (HF, MP2, DFT) with a series of basis sets and analyzed in comparison with similar data for 2PBI and compared to experimental data when appropriate. The hybrid density functionals used in our investigation have demonstrated very good performance for a prediction of molecular structure and vibrational spectra of similar organic molecules [12, 14–16].

Experimental

2-(2′-Pyridyl)benzimidazole (2PBI) and 1-methyl 2-(2′-pyridyl)benzimidazole (Me2PBI) have been synthesized in the Laboratory of Bioactive Organic Compounds (Department of Chemistry, Lomonosov Moscow State University) and had a purity about 98 %. The FT-IR spectra of both compounds pelleted with KBr have been recorded in the Laboratory of Molecular Spectroscopy using Tensor-27 (Bruker) set with resolution ± 1 cm^{-1}. The FT-Raman spectra have been registered on an Equinox-55 Bruker interferometer equipped with FRA-106 Raman accessory in the 3500–100 cm^{-1} Stokes region using 1064-nm line of an Nd:YAG laser for excitation operating at 200–500 mW power. Raman spectra were recorded from the pure powders in a backscattering geometry; the signal was averaged upon 200 scans. The reported wave numbers are believed to be accurate within ± 2 cm^{-1}.

Computational details

Ab initio and DFT calculations have been performed with the Gaussian 03 (Revision E.01) [17] and Gaussian 09 (Revision A.01) [18] packages. The fully optimized geometries and harmonic force fields of Me2PBI possible isomers have been calculated at the HF, MP2 and B3LYP [19–22] levels of theory with 6-31G*, 6-31+G* and 6-31+G** basis sets [23, 24]. The optimized geometries of the most stable conformations of Me2PBI and 2PBI have been confirmed by calculations at the MP2/TZVP and BVP86/TZVP [25] levels of theory using R. Ahlrichs et al. triple-ζ basis set [26, 27]. All calculations have been done without any restrictions on the symmetry of structure. The influence of solvent environment on structure and vibrational spectra of Me2PBI has been considered within the CPCM polarizable conductor calculation model [28, 29] for water and dimethylformamide as solvents which are usually used in investigations of systems containing 2PBI and its derivatives. The accuracy of self-consistent reaction field (SCRF) model in predicting the structure and

energetics of a series of organic molecules has already been well confirmed elsewhere.

The minima of the potential surface were found by relaxing the geometric parameters with the standard optimization methods. Analytical force constants have been derived, and harmonic vibrational frequencies have been calculated at all aforementioned theoretical levels to confirm the nature of stationary points found and to account for the zero-point vibrational energy (ZPE) correction. Torsional potential energy curves of Me2PBI and 2PBI molecules (in gaseous state and in water and DMF solutions) for the rotation around the central (pivotal) C–C bond in the 0°–360° rotation range have been obtained by varying the torsion angle φ = N1–C1–C2–N3 in steps of 10° starting from the most stable A conformations and fully optimizing the molecular geometry and calculating vibrational frequencies at each point. Comparison of potential curves for gaseous and solvated (aqueous) Me2PBI is performed in Fig. 2. Figure 3 presents results of similar calculations of 2PBI molecule.

The visualization of theoretical IR spectra has been made using Chemcraft (version 1.6) software [30] with the Lorentzian broadening, the half bandwidth has been taken as equal to ~5–8 cm^{-1}. The prediction of Raman intensities was carried out by the following procedure: The Raman activities calculated by Gaussian 09 were converted to relative Raman intensities using well-known relation from the basic theory of Raman scattering [31] and then were visualized by the original software Curves [32].

Normal coordinate analysis has been performed in the local symmetry coordinates. The numbering of atoms is presented in Fig. 4, and the introduced internal coordinates of Me2PBI molecule are illustrated in Fig. 4S. The redundant sets of internal coordinates of Me2PBI molecules include 103 internal coordinates: all bond stretches,

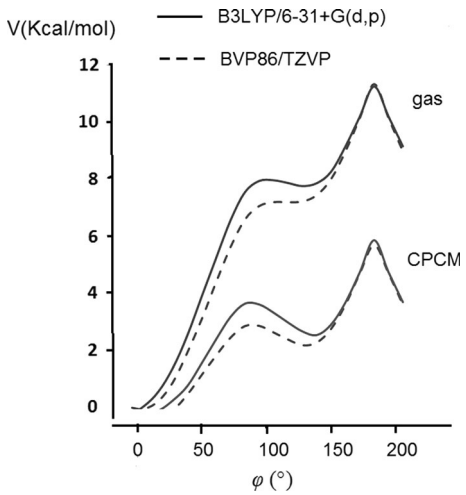

Fig. 2 Torsional potentials of 1-methyl 2-(2′-pyridyl)benzimidazole

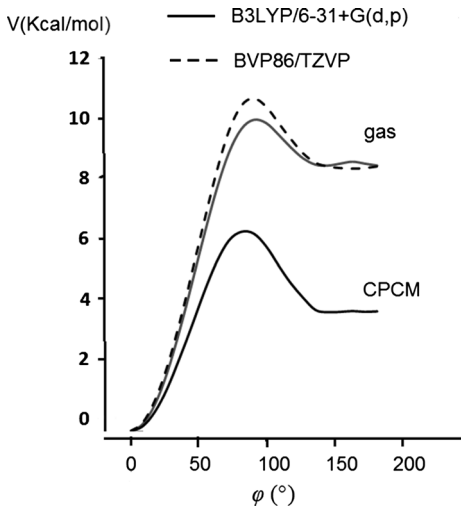

Fig. 3 Torsional potentials of 2-(2′-pyridyl)benzimidazole

bond angles, out-of-plane and torsional coordinates. From this set, a non-redundant set of local symmetry coordinates was constructed. The local symmetry of the disubstituted benzene ring could be approximately considered as C_{2v}, and corresponding coordinates were constructed as in Refs. [33, 34]; local symmetry coordinates related to central part with ordinary C–C bond were defined in accordance with the local C_s symmetry. Local coordinates related to the pyridine ring were chosen similar to proposed in [35] for 3-methylpyridine, and local coordinates for imidazole ring were constructed in the same way as in Ref. [34] for the benzimidazole molecule. The butterfly-type deformation coordinates have been chosen as a combination of two torsional coordinates. The local coordinates of the methyl group were defined within C_{3v} symmetry (see supporting materials).

The software package SPECTRUM [36–40] has been used for transformation of quantum mechanical Cartesian force constants to the force constant matrix in redundant internal coordinates in the frame of the canonical matrix model [41]. A part of diagonal force constants in redundant system of internal coordinates is displayed in supporting information. Normal coordinate analysis for all investigated molecules has been carried out using SPECTRUM; potential energy distributions have been calculated in accordance with formula from Ref. [42].

Results and discussion

Optimized conformations and energetics

The relative energies of Me2PBI conformations calculated at different levels of theory in gaseous state and in water and DMF solutions are reported in Table 1, and

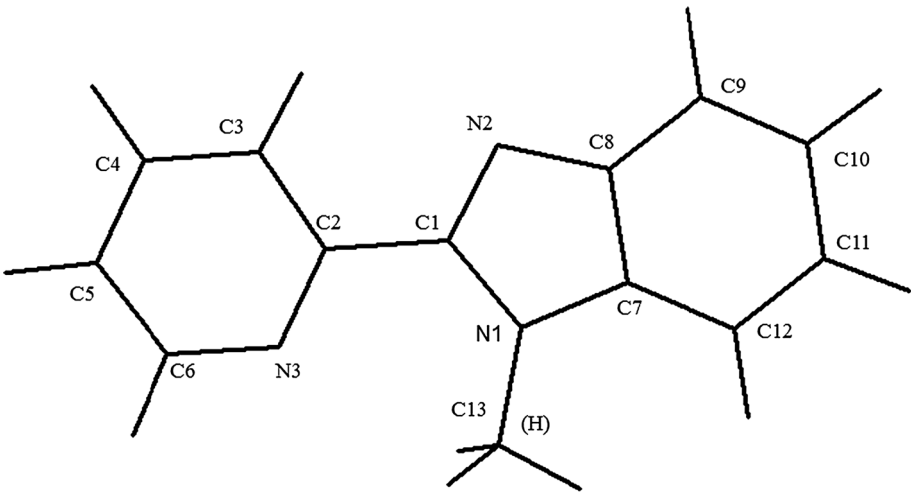

Fig. 4 Numbering of atoms of 1-methyl 2-(2′-pyridyl) benzimidazole molecule

comparison of optimized B3LYP/6-31+G(d,p) geometries for the skeleton of Me2PBI and corresponding force constants is presented in Table 2.

According to the results of calculations, the relative stabilities of Me2PBI conformations in the presence of solvents are the same as of isolated molecules, but the energy difference between conformations has decreased in comparison with gaseous state. 2PBI-A-conformation is also the most stable in solvated form. The values of ZPE corrected energy differences between Me2PBI-A and Me2PBI-B forms are equal to 2.1 kcal/mol in H_2O and 2.3 kcal/mol in DMF so the concentrations of form B in both solvents should be rather low. The relative energy of tautomeric Me2PBI (form C) in solvents remains very large, and this result is in good correspondence with conclusions on the conformational stability of 2PBI molecule [11]. Optimized Me2PBI-A molecule in gas has a plane of symmetry and belongs to the C_S point symmetry group. The Me2PBI-B structure is non-planar with dihedral angle N1–C1–C2–N3 equal to $\sim 54°$.

The conformation Me2PBI-A is the most stable in all calculations, and optimized geometry parameters of both conformations skeletons are very close to the optimized geometry of 2PBI conformers in gaseous and in aqueous states [12, 13]. The experimental investigations of Me2PBI structure are not available, and we use the X-ray data of 2PBI [13] as the reference data. The optimized B3LYP/6-31+G(d,p) bond lengths of 2PBI are very similar in both A and B conformations and are mostly in good accordance with experimental structure parameters (taking into account the difference in physical states). The lengths of all skeleton bonds in A and B conformations of 2PBI and Me2PBI are similar, except the pivotal C1–C2 bond, where the difference in length is about 0.01 Å between A and B forms and 0.04 Å between A and C forms. The presence of CH_3 group in the imidazole ring leads to the elongation of the pivotal bond in all forms of Me2PBI with respect to the corresponding structures of 2PBI. The force constants of C–C bonds in different structures are decreased upon the elongation of the bond, and this change in geometry should lead to the slight redshift of corresponding stretching frequency.

The data in Table 2 demonstrate the strong similar trends in values of optimized geometry parameters and

Table 1 ZPE corrected relative energies (in kcal/mol) for stable conformations of 2-(2′-pyridyl)benzimidazole and 1-methyl 2-(2′-pyridyl) benzimidazole

Compound	B3LYP/6-31+G**			M062X/6-31+G**	BVP86/TZVP
	Gas	CPCM H_2O	CPCM DMF	Gas	Gas
Me2PBI					
A	0.0	0.0	0.0	0.0	0.0
B	6.6	2.1	2.3	6.7	7.2
C	20.2	19.6	15.7	24.7	19.8
2PBI					
A	0.0	0.0	0.0	0.0	0.0
B	9.2	3.1	4.3	9.6	9.5
C	19.7	10.9	12.4	22.8	17.1

Table 2 Optimized B3LYP/6-31+G** geometry of skeletons (bond lengths in Å, bond angles in degrees) and diagonal force constants (F, in mdyn×Å, mdyn) for corresponding internal coordinates of 2PBI and Me2PBI

Parameter	2PBI X-ray [13]	2PBI-A		2PBI-B		2PBI-A (CPCM, H_2O)		Me2PBI-A (gas)		Me2PBI-A (CPCM, H_2O)		Me2PBI-B (gas)	
		R_e	F	R_e	F	R_e	F	R_e	F	R_e	F	R_e	F
C1–N1 Qi5	1.355(2)	1.376	4.419	1.389	4.007	1.372	4.349	1.389	4.273	1.382	4.340	1.392	3.948
C1–N2 Qi1	1.317(2)	1.319	5.592	1.314	5.672	1.324	5.382	1.324	5.756	1.327	5.541	1.314	5.642
C1–C2 QQ	1.466	1.466	5.451	1.475	5.167	1.469	5.325	1.473	5.300	1.479	5.114	1.484	4.857
C2–N3 Qp1	1.336	1.347	5.549	1.344	5.544	1.348	5.503	1.348	5.560	1.348	5.450	1.344	5.365
C2–C3 Qp6	1.377	1.403	4.992	1.406	4.895	1.402	4.975	1.404	4.874	1.404	4.946	1.404	4.774
C3–C4 Qp5	1.372	1.392	5.534	1.394	5.475	1.393	5.468	1.394	5.587	1.394	5.468	1.394	5.457
C4–C5 Qp4	1.364	1.398	5.344	1.394	5.454	1.397	5.347	1.397	5.371	1.397	5.371	1.393	5.460
C5–C6 Qp3	1.366	1.397	5.094	1.399	5.027	1.398	5.069	1.397	5.154	1.397	5.090	1.398	5.062
N3–C6 Qp2	1.328	1.338	5.820	1.335	5.859	1.339	5.742	1.341	5.749	1.341	5.684	1.337	5.614
N1–C7 Qi4	1.355	1.379	4.689	1.383	4.636	1.379	4.654	1.385	4.754	1.385	4.675	1.385	4.481
N2–C8 Qi2	1.389	1.384	4.165	1.383	4.142	1.386	4.126	1.383	4.473	1.383	4.314	1.383	4.076
C7–C8 Qbi	1.394	1.421	3.264	1.418	3.298	1.420	3.290	1.415	3.684	1.415	3.684	1.416	3.505
C8–C9 Qb1	1.396	1.403	5.105	1.403	5.110	1.404	5.061	1.404	5.176	1.404	5.176	1.402	5.184
C9–C10 Qb2	1.368	1.392	5.388	1.392	5.381	1.393	5.336	1.393	5.424	1.393	5.424	1.392	5.398
C10–C11 Qb3	1.392	1.413	5.094	1.413	4.728	1.414	4.670	1.414	4.815	1.414	4.815	1.412	4.832
C11–C12 Qb4	1.376	1.394	5.343	1.394	5.330	1.394	5.304	1.395	5.453	1.395	5.379	1.395	5.356
C7–C12 Qb5	1.387	1.398	5.183	1.398	5.188	1.399	5.146	1.400	5.238	1.400	5.238	1.399	5.231
∠N1–C1–N2	113.1(16)	113.0	0.847	112.5	0.815	112.8	0.816	112.7	0.859	112.7	0.873	113.2	0.850
∠N1–C1–C2–N3	13.0	0.0		154.7		0.0		0.2		32.4		128.6	
∠N2–C1–C2–N3	167.4	180.0		26.9		180.0		179.8		152.8		54.1	

Numbering of atoms is given in Fig. 4

corresponding force constants of both compounds in gaseous state, while most of these parameters are slightly changed in water surrounding. The significant influence of solvent on the geometry was observed for the pivotal (central) C–C bond in 2PBI-C molecule [14], and the same result is obtained for Me2PBI-C conformation, where the length of pivotal bond is increased (by ~0.02–0.03 Å) in both solvents in comparison with isolated molecules. The influence of methyl group on geometry of Me2PBI in comparison with 2PBI is practically negligible except the slight elongation (~0.01–0.015 Å) of skeleton bonds adjusted to CH_3 group and C1–N2 imidazole bond near pivotal C–C bond of Me2PBI-A, and also shortening two other bonds of imidazole group. Geometry of pyridine and benzene groups is practically not altered as well as force constants of these groups. Correspondingly, one can suppose the slight differences in vibrational spectrum of both compounds.

The B3LYP/6-31+G(d,p) torsional curve of Me2PBI in the gaseous state (upper solid curve in Fig. 2) has only one definite minima at $\varphi = 0°$ corresponding to the conformation A with planar skeleton. The stable conformations (B) are calculated at three rotation angles near 110°, 120° and 130° which have almost constant potential energy (within 0.1 kcal/mol). The optimized conformation of Me2PBI-B at this level of theory corresponds to $\varphi = 128.6°$. Optimized conformations of Me2PBI in this interval have slightly different lowest frequencies, but in general their theoretical IR curves are very similar. The barrier height of B → B transition at $\varphi = 180°$ is about 3.6 kcal/mol.

The BVP86/TZVP torsional curve (upper dotted curve in Fig. 3) has the minimum at $\varphi = 10.0°$ corresponding to the form A, while the second stable conformation (B) corresponds to the more noticeable minimum at 130° (similar to the B3LYP calculations). Barrier height of B → A transition is equal to 0.2 kcal/mol at $\varphi = 110°$. Barrier height for A → A transition (at $\varphi = 0°$) near the first minimum is about 0.12 kcal/mol. So, analysis of these two torsional curves allows us to conclude that the form A should be the most probable stable conformation in the gaseous Me2PBI.

According to CPCM calculations, the same conformation is also the most stable one of the solvated Me2PBI (Fig. 2, bottom curves), and it is stabilized near $\varphi = 20°$ and 30° at BVP86/TZVP and B3LYP/6-31+G(d,p) levels,

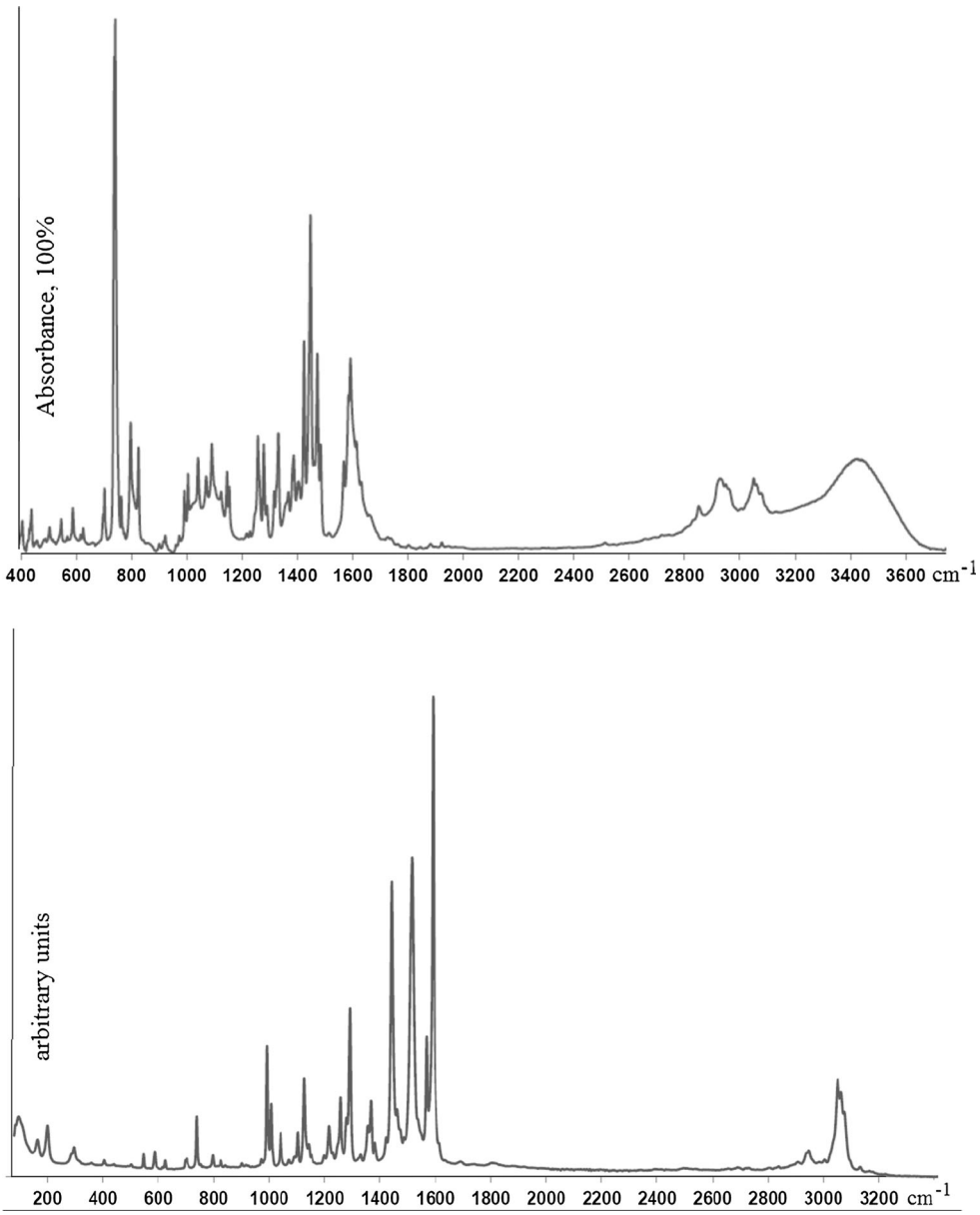

Fig. 5 Infrared (*top*) and Raman (*bottom*) spectra of 1-methyl 2-(2′-pyridyl)benzimidazole

respectively. The minimum that corresponded to form B is observed near 130° and 130–140° at B3LYP/6-31+G(d,p) and BVP86/TZVP levels, respectively. The barriers of A → A transition at $\varphi = 0°$ are equal to 0.2 and 0.1 kcal/mol in the B3LYP and BVP86 calculations, respectively.

For comparison, we perform the potential curves of 2PBI (Fig. 3) calculated at the same two levels of theory for gaseous state and at B3LYP/6-31+G(d,p) level for CPCM model. These curves are different from similar ones of Me2PBI: Both curves of gaseous 2PBI (top curves) have two evident maxima near $\varphi = 100°$ and 260°. The barrier height of B → A transition at $\varphi = 100°$ is about 1.5 kcal/mol. At the B3LYP level, the third small maximum is observed near $\varphi = 180°$ with barrier height about 0.15 kcal/mol. In the presence of water (bottom curve), only two maxima are observed with the barrier height of B → A transition increased up to 2.7 kcal/mol. Four B-conformers of 2PBI optimized in interval 150–180° have practically the same total energies which vary within 0.04 kcal/mol. Obviously the hindered internal rotation in both compounds is complicated function, and more developed models should be applied for its analysis. Another factor that should be considered is a large anharmonicity and connected with this a possibility of large amplitude torsional motion in both compounds. Possibly, in definite conditions, the conformation 2PBI-B could exist in noticeable concentrations.

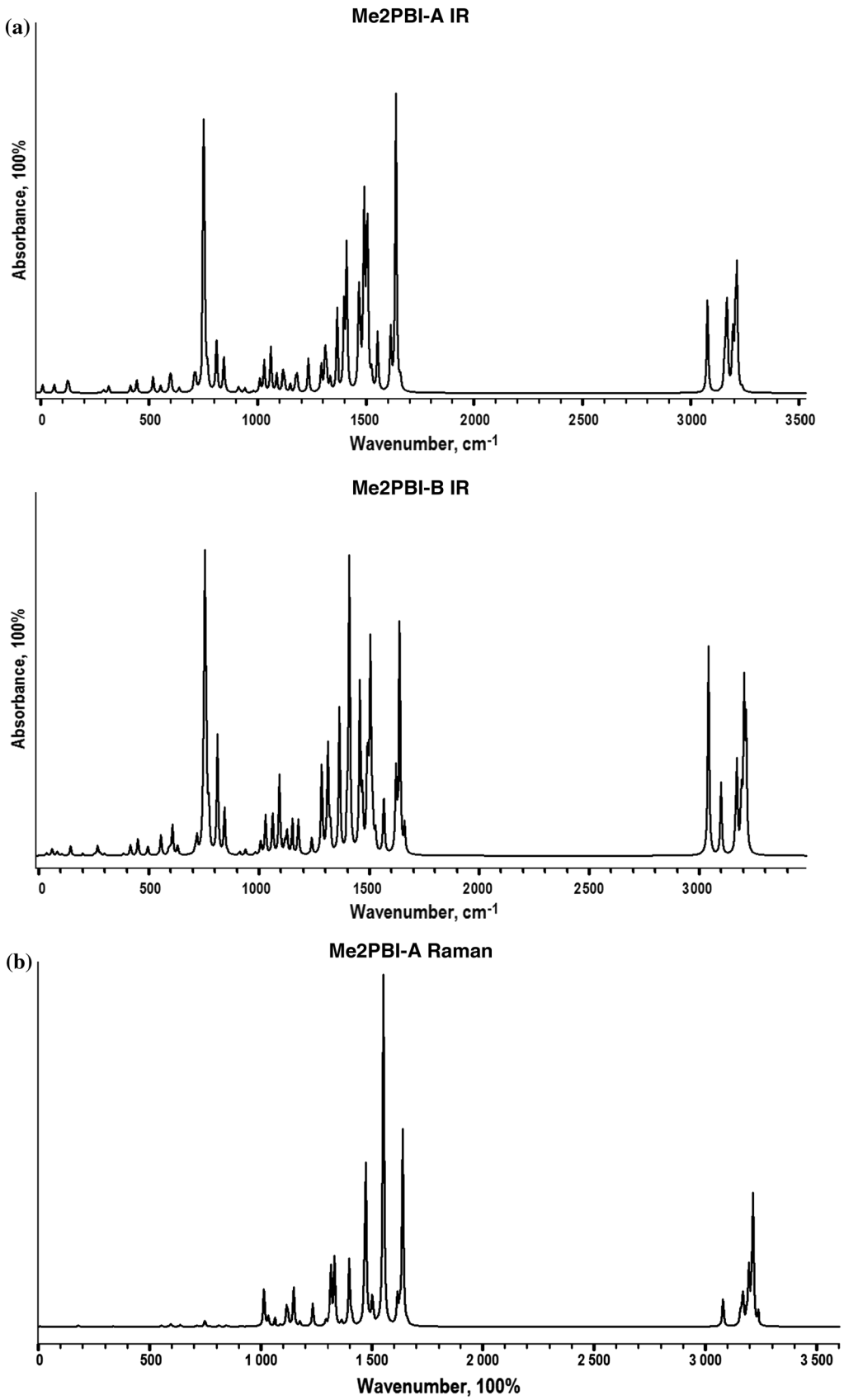

Fig. 6 Theoretical (B3LYP/6-31+G(d,p) infrared (**a**) and Raman (**b**) spectra of conformations A and B of 1-methyl 2-(2′-pyridyl)benzimidazole

Fig. 6 continued

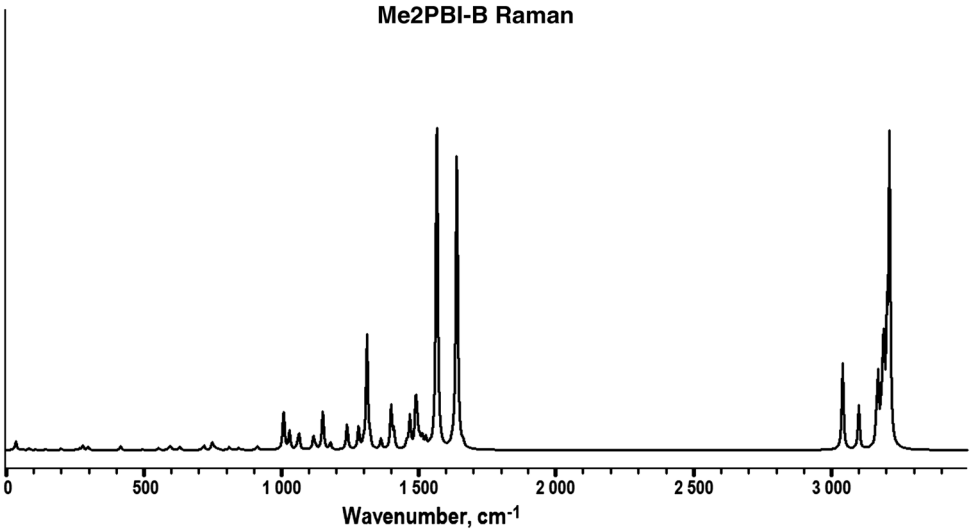

Vibrational spectra, normal coordinate analysis

IR and Raman spectra of Me2PBI are presented in Fig. 5. The wavenumbers of registered IR and Raman spectra of 2MePBI in comparison with theoretical vibrational frequencies, IR intensities and Raman activities are presented in Table S2. Visualized theoretical vibrational spectra of Me2PBI-A and Me2PBI-B conformations are presented in Fig. 6.

From comparison of theoretical and experimental frequencies (Table S2), one can see that for some vibrational modes, chosen approach results in larger deviations of calculated frequencies from experimental spectra, and this effect could be due to the anharmonicity of experimental frequencies. To determine the empirical correction of the theoretical data, the scaling procedure in Cartesian coordinates [43] has been applied. The B3LYP/6-31+G(d,p) scaling factors of model molecules—pyridine, *N*-methylimidazole and benzimidazole (with complete sets of fundamentals given in [44–46], respectively)—have been calculated and used for correction theoretical frequencies of Me2PBI-A and Me2PBI-B conformations. Experimental error δ was chosen to be ± 3 cm^{-1} for each frequency. The scaling ab initio force field matrix in Cartesian coordinates allows us to avoid introducing internal coordinates in this step which is necessary part of the well-known scaling scheme where initially we need to transform the QM force field to internal coordinates. The posing of inverse vibrational problem proposed in Ref. [47–49] has been used in the scale factor optimization. We search for a force constant matrix F in Cartesian coordinates (defined through the scaling factors) that is the nearest (in a sense of Euclidian norm) to matrix F^0 and reproduces the set of experimental data Λ_δ within given error level $\delta \geq 0$. Such solution could be found using stable numerical methods within the confines of the Tikhonov regularization theory [41, 43]. Optimized values of scaling factors are presented in supporting materials.

After scaling in Cartesian coordinates, the corrected force constant matrices of Me2PBI have been transformed from Cartesian to redundant internal coordinates and finally to local symmetry coordinates. Scaled frequencies and potential energy distributions in local symmetry coordinates are also presented in Table S2. On a base of calculated potential energy distribution in local symmetry coordinates, the interpretation of experimental IR and Raman spectra has been proposed (Table S2). The comparison of scaled frequencies with experimental data and results of similar calculations of 2PBI [14] confirms the possibility of using scaling procedure in Cartesian coordinates for the correction of harmonic calculations.

The tentative assignment for the most vibrations of Me2PBI can be proposed based on comparison between observed and theoretical spectra, except the lowest frequencies (Table S2). One should note that here we compare the theoretical results obtained for the gaseous phase and experimental spectra registered for the solid state. Nevertheless, there is a good correspondence between scaled theoretical and observed frequencies. The theoretical B3LYP/6-31+G(d,p) IR intensities and Raman activities (Table S2) adequately reflect the experimental shapes.

Consider the main characteristic frequencies for both compounds that are important for compound identification. Appearance of a broadband in the 3400–3450 cm^{-1} region in IR spectrum of Me2PBI could be explained by possible influence of water molecules associated with Me2PBI [14]. One of the main differences between experimental IR spectra of 2PBI and Me2PBI is an occurrence of very broad complicated shape band in the 2500–3200 cm^{-1} region in IR spectrum of 2PBI, which is absent in the Me2PBI IR

spectrum. This region in the IR spectrum of 2PBI is very similar to the IR spectrum of the hydrogen bonded imidazole crystal (so-called imidazole N–H effect) when the presence of this complicated band is explained by the statistical disorder in crystalline lattice, due to bending of the H-bonds [50–52]. Similar strong coupling effects have also been observed in IR spectra of crystals with strong O–H…O bonds for some other compounds [53, 54]. A pair of intensive bands near 1467 and 1443 cm^{-1} in IR spectrum of 2PBI have the counterparts in IR spectrum of Me2PBI at 1471 and 1447 cm^{-1} both assigned to the CH in-plane bending of Py fragment. Specific spectral feature of both compounds includes an appearance of very strong IR band near 745 cm^{-1} (2PBI) and 741 cm^{-1} (Me2PBI). Based on PED calculations, these bands can be assigned to the CH out-of-plane bending of imidazole fragment with large contribution of out-of-plane deformations of pyridyl ring. Corresponding theoretical IR bands are at 754 and 756 cm^{-1} for 2PBI-A [14] and Me2PBI-A (Table S2). This assignment is well correlated with proposed elsewhere for pyridine molecule [44]. Theoretical IR spectra of conformations B also contain intensive bands near 750 cm^{-1} which are assigned to the same vibration, but, in general, theoretical IR and Raman curves of conformations B are in worse correspondence with experimental spectra, especially in the "fingerprint" region. The 400–700 cm^{-1} IR region can be defined as informative for the separation between A and B forms (Fig. 7): One can see the better correspondence between the observed and calculated IR spectra for form A rather than for form B.

Consider the influence of the CH_3 substitution on the geometry and spectral properties of the pivotal C–C bond. According to the calculations, this CC stretching should have very intensive line in Raman spectrum and almost zero-intensity band in the IR spectrum. We can assign to this vibration the strong bands near 1538 and 1518 cm^{-1} in the Raman spectra of 2PBI and Me2PBI, respectively. This assignment confirms the conclusion made on a base of comparison of theoretical bond lengths and force constants of two compounds (Table 2) about the slight redshift of this vibration in vibrational spectrum of Me2PBI. Analysis of experimental and theoretical data allows us to conclude that the position of most frequencies remains characteristic and does not strongly depend on the configuration and electronic structure of these molecules.

Comparing theoretical spectra of two Me2PBI conformations, one can see very close values of theoretical frequencies of both conformations and the absence of very apparent differences in both IR and Raman spectra except the 400–700 cm^{-1} region in IR spectra (Fig. 7) where the theoretical IR spectrum of form A is in better correspondence with observed spectrum.

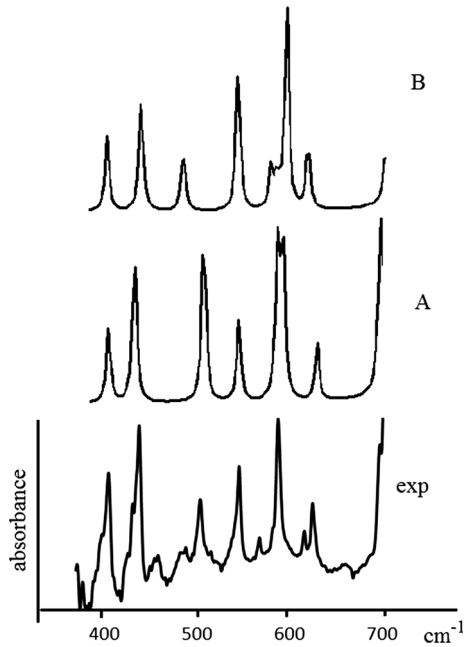

Fig. 7 Experimental and theoretical (B3LYP/6-31+G(d,p)) IR spectra of 1-methyl 2-(2′-pyridyl)benzimidazole A and B conformations in the 400–700 cm^{-1} region

In general, IR spectra are more preferable for the identification of 2PBI and Me2PBI compounds. The main differences between experimental 2PBI and Me2PBI IR spectra are observed near 1300 cm^{-1}. The IR spectrum of 2PBI contains very intensive bands at 1280 and 1315 cm^{-1} which according to PED calculation can be assigned to CC stretching and CH in-plane-bending vibrations of the benzene fragment, respectively [14], while the same regions in observed and theoretical IR spectra of 2Me2PBI have no corresponding intensive bands (see Fig. 6a). Raman spectra of both compounds are very similar, and one exception is the appearance of a weak line near 2950 cm^{-1} in the spectrum of Me2PBI related to the CH stretching of methyl group. The comparison of experimental and theoretical IR and Raman spectra of 2PBI and Me2PBI around 700–1600 cm^{-1} allows us to conclude that the A conformations are energetically preferred in solid 2PBI and Me2PBI. Theoretical IR and Raman spectra of 2PBI(A) and Me2PBI(A) well correlate with the experimental spectra, taking into account the aggregate state of investigated samples.

Conclusions

Infrared and Raman spectra of Me2PBI have been studied by spectral measurements and DFT (B3LYP/6-31+G**) calculations for all possible conformations. Both experimental and theoretical investigations of Me2PBI have been

carried out for the first time. Based on the complete assignment of vibrational spectra of both compounds with help of potential energy distribution, we can conclude that broad complicated band in the 2500–3200 cm^{-1}, two bands near 1280 and 1315 cm^{-1} and band near 745 cm^{-1} in the IR spectrum of 2PBI assigned to vibrations of imidazole fragment are the main distinguishable markers between two compounds because they are absent in the IR spectrum of Me2PBI. The relative stability of conformations is similar for both compounds, and the most part of vibrational frequencies does not depend on methyl substitution. Both 2PBI and Me2PBI in solid state at ambient temperature exist as more stable A-conformations. Results of calculations within PCM models demonstrate the strong dependence of the relative stability of A and B structures of both compounds on the solvent. The empirical correction of theoretical force fields of 2PBI and Me2PBI, with a help of scaling procedure in Cartesian coordinates, has demonstrated good agreement of theoretical frequencies with the experimental ones.

Acknowledgments This work was partially supported by the RFBR Grant No. 14-03-00929a. J.L. and L.G.G. acknowledge the support from National Science Foundation (NSF) for Interdisciplinary Center for Nanotoxicity (ICN) through CREST Grant HRD-0833178 and NSF-PREM Grant DMR-1205194.

References

1. Prieto FR, Mosquera M, Novo M (1990) J Phys Chem 94:8536
2. Novo M, Mosquera M, Prieto FR (1993) J Chem Soc Faraday Trans 89:885
3. Novo M, Mosquera M, Prieto FR (1992) Can J Chem 70:823
4. Novo M, Mosquera M, Prieto FR (1995) J Phys Chem 99:14726
5. Kondo M (1978) Bull Chem Soc Jpn 51:3027
6. Brown RG, Entwistle N, Hepworth JD, Hodgson KW, May BJ (1982) J Phys Chem 86:2418
7. Mukherjee TK, Ahuja P, Koner AL, Datta A (2005) J Phys Chem B 109:12567
8. Munuera C, Barrena E, Ocal C (2005) Langmuir 21:8270
9. Uznański P, Kurjata J, Bryszewska E (2009) Mater Sci Pol 27:659
10. Kamat PV (2002) J Phys Chem B 106:7729
11. Lane TJ, Nakagawa I, Walter JL, Kandathil J (1962) Inorg Chem 1:267
12. Guin M, Maity S, Patwari GN (2010) J Phys Chem A 114:8323
13. Likhanova NV, Veloz MA, Hopfi H, Matias DJ (2007) J Heterocycl Chem 44:145
14. Vakula OA, Vakula NI, Kuramshina GM, Pentin YA (2013) Russ J Phys Chem A 87:1527
15. Kosenkov D, Kholod YA, Gorb L, Shishkin OV, Kuramshina GM, Dovbeshko GI, Leszczynski J (2009) J Phys Chem A 113:9386
16. Carbonierre P, Barone V (2004) Chem Phys Lett 399:226–229
17. Frisch MJ, Trucks GW, Schlegel HB, Scuseria GE, Robb MA, Cheeseman JR, Montgomery JA Jr, Vreven T, Kudin KN, Burant JC, Millam JM, Iyengar SS, Tomasi J, Barone V, Mennucci B, Cossi M, Scalmani G, Rega N, Petersson GA, Nakatsuji H, Hada M, Ehara M, Toyota K, Fukuda R, Hasegawa J, Ishida M, Nakajima T, Honda Y, Kitao O, Nakai H, Klene M, Li X, Knox JE, Hratchian HP, Cross JB, Bakken V, Adamo C, Jaramillo J, Gomperts R, Stratmann RE, Yazyev O, Austin AJ, Cammi R, Pomelli C, Ochterski JW, Ayala PY, Morokuma K, Voth GA, Salvador P, Dannenberg JJ, Zakrzewski VG, Dapprich S, Daniels AD, Strain MC, Farkas O, Malick DK, Rabuck AD, Raghavachari K, Foresman JB, Ortiz JV, Cui Q, Baboul AG, Clifford S, Cioslowski J, Stefanov BB, Liu G, Liashenko A, Piskorz P, Komaromi I, Martin RL, Fox DJ, Keith T, Al-Laham MA, Peng CY, Nanayakkara A, Challacombe M, Gill PMW, Johnson B, Chen W, Wong MW, Gonzalez C, Pople JA (2004) Gaussian 03, Revision E.01. Gaussian, Inc., Wallingford
18. Frisch MJ, Trucks GW, Schlegel HB, Scuseria GE, Robb MA, Cheeseman JR, Scalmani G, Barone V, Mennucci B, Petersson GA, Nakatsuji H, Caricato M, Li X, Hratchian HP, Izmaylov AF, Bloino J, Zheng G, Sonnenberg JL, Hada M, Ehara M, Toyota K, Fukuda R, Hasegawa J, Ishida M, Nakajima T, Honda Y, Kitao O, Nakai H, Vreven T, Montgomery JA Jr, Peralta JE, Ogliaro F, Bearpark M, Heyd JJ, Brothers E, Kudin KN, Staroverov VN, Kobayashi R, Normand J, Raghavachari K, Rendell A, Burant JC, Iyengar SS, Tomasi J, Cossi M, Rega N, Millam JM, Klene M, Knox JE, Cross JB, Bakken V, Adamo C, Jaramillo J, Gomperts R, Stratmann RE, Yazyev O, Austin AJ, Cammi R, Pomelli C, Ochterski JW, Martin RL, Morokuma K, Zakrzewski VG, Voth GA, Salvador P, Dannenberg JJ, Dapprich S, Daniels AD, Farkas O, Foresman JB, Ortiz JV, Cioslowski J, Fox DJ (2009) Gaussian 09, Revision A.01. Gaussian, Inc., Wallingford
19. Roothaan CCJ (1951) Rev Mod Phys 23:69
20. Becke AD (1993) J Chem Phys 98:5648
21. Adamo C, Barone V (1999) J Chem Phys 110:6158
22. Lee C, Yang W, Parr RG (1988) Phys Rev B 37:785
23. Jensen F (1999) Introduction to computational chemistry. Wiley, Chichester, p 446
24. Yang Yue, Weaver MN, Merz KM Jr (2009) J Phys Chem A 113:9843
25. Becke AD (1988) Phys Rev A 38:3098
26. Schaefer A, Horn H, Ahlrichs R (1992) J Chem Phys 97:2571
27. Schaefer A, Huber C, Ahlrichs R (1994) J Chem Phys 100:5829
28. Barone V, Cossi M (1995) J Phys Chem A 1998:102
29. Cossi M, Rega N, Scalmani G, Barone V (2003) J Comput Chem 24:669
30. ChemCraft (Version 1.6). http://www.chemcraftprog.com
31. Krishnakumar V, Keresztury G, Sundius T, Ramasamy R (2002) J Mol Struct 702:9
32. Kochikov IV, Kuramshina GM, Samkov LM, Sharapov DA, Sharapova SA (2007) Numer Methods Program 8:70
33. Shimojima A, Takahashi H (1993) J Phys Chem 97:9103
34. Krishnakumar V, Ramasamy R (2005) Spectrochim Acta Part A 62:570
35. López-Tocón I, Woolley MS, Otero JC, Marcos JI (1998) J Mol Struct 470:241
36. Kochikov IV, Kuramshina GM (1985) Vestnik Moskovskogo Universiteta, Seriya 2. Khimiya 26:354
37. Kochikov IV, Yagola AG, Kuramshina GM, Kovba VM, Pentin YA (1985) Spectrochim Acta 41A:185
38. Yagola AG, Kochikov IV, Kuramshina GM, Pentin YA (1999) Inverse problems of vibrational spectroscopy. VSP, Zeist
39. Kochikov IV, Tarasov YI, Spiridonov VP, Kuramshina GM, Saakjan AS, Yagola AG (2000) J Mol Struct 550–551:429
40. Kochikov IV, Tarasov YI, Spiridonov VP, Kuramshina GM, Yagola AG, Saakjan AS, Popik MV, Samdal S (1999) J Mol Struct 485–486:421
41. Kuramshina GM, Weinhold FA, Kochikov IV, Pentin YA, Yagola AG (1994) J Chem Phys 100:1414
42. Kerestury G, Jalkovsky G (1971) G. J Mol Struct 10:304

43. Kochikov IV, Kuramshina GM, Stepanova AV (2009) Int J Quant Chem 109:28
44. Wong KN, Coulson SD (1984) J Mol Spectrosc 104:129
45. Perchard C, Novak A (1953) Spectrochim Acta 1967:27A
46. Klots TD, Devlin P, Collier WB (1997) Spectrochim Acta Part A 53:2445
47. Kochikov IV, Kuramshina GM, Stepanova AV, Yagola AG (2004) Numer Methods Program 5:281
48. Goncharsky AV, Leonov AS, Yagola AG (1974) Dokl Akad Nauk SSSR 214:499
49. Kochikov IV, Kuramshina GM, Pentin YA, Yagola AG (1987) USSR Comput Math Math Phys 27:33
50. Goodman L, Ozkabak AG, Thakur SN (1991) J Phys Chem 95:9044
51. Excoffon P, Marechal Y (1980) Chem Phys 52:237
52. Flakus HT, Bryk A (1996) J Mol Struct 372:215
53. Vener MV, Egorova AN, Churakov AV, Tsirelson VGJ (2012) Comput Chem 33:2303
54. Churakov AV, Prikhodchenko PV, Lev O, Medvedev AG, Tipol'skaya TA, Vener MV (2010) J Chem Phys 133:164506